Gate-Controlled Superconductivity in a Diffusive Multiwalled Carbon Nanotube

T. Tsuneta,[1] L. Lechner,[1,2] and P. J. Hakonen[1]

[1]*Low Temperature Laboratory, Helsinki University of Technology, Otakaari 3A, Espoo, 02015 Finland*

[2]*Institute for Experimental and Applied Physics, University of Regensburg, Universitätsstr. 31, D-93040 Regensburg, Germany*

(Received 5 September 2006; published 21 February 2007; corrected 26 February 2007)

We have investigated electrical transport in a diffusive multiwalled carbon nanotube contacted using superconducting leads made of an Al/Ti sandwich structure. We find proximity-induced superconductivity with measured critical currents up to $I_{cm} = 1.3$ nA, tunable by the gate voltage down to 10 pA. The supercurrent branch displays a finite zero bias resistance which varies as $R_0 \propto I_{cm}^{-\alpha}$ with $\alpha = 0.74$. Using IV characteristics of junctions with phase diffusion, a good agreement is obtained with the Josephson coupling energy in the long, diffusive junction model of A. D. Zaikin and G. F. Zharkov [Sov. J. Low Temp. Phys. **7**, 184 (1981)].

DOI: 10.1103/PhysRevLett.98.087002 PACS numbers: 74.70.Wz, 74.78.Na

Superconductivity in carbon nanotubes is an intriguing subject. To understand it one has to consider many facets of modern physics, including Luttinger liquid behavior owing to strong electron-electron interactions in one dimension as well as Kondo physics due to odd, unpaired electronic spin [1]. Proximity-induced and intrinsic superconductivity has been observed in individual and bundled single walled carbon nanotubes (SWNT) [2–6]. The magnitude of observed supercurrents has varied substantially. In Refs. [3,4], respectively, a supercurrent on the order of 10× larger and 10× smaller than theoretically expected was observed. Morpurgo *et al.* [5] and Jorgensen *et al.* [6], on the other hand, did observe only increased conductance near zero bias.

In multiwalled carbon nanotubes (MWNT), supercurrents have been even harder to achieve, presumably due to problems with disorder and impurities. Enhanced conductance was observed by Buitelaar *et al.* [7] near zero bias, which was interpreted in terms of multiple Andreev reflections (MAR) in the presence of inelastic processes [8]. Similar results were obtained by Kasumov *et al.* [3]. Recently a proximity-induced supercurrent was observed by Haruyama and co-workers [9,10], most notably in multi-shell-contacted tubes grown within nanoporous alumina templates [10]. Here we report proximity-induced superconductivity that is achieved in an individual, diffusive MWNT bulk(side) contacted with Ti/Al contacts. We find that the supercurrent can be smoothly controlled by gate voltage, via tuning of the diffusion constant, and a good agreement is obtained using analysis based on long, diffusive S-NS junctions supplemented with phase-diffusion effects, modeled in terms of the resistively and capacitively shunted junction model (RCSJ).

Our tube material, provided by the group of S. Iijima, was grown using plasma enhanced growth without any metal catalyst [11]. The absence of a catalyst (which is often Ni or Fe) guarantees that our tubes do not have any magnetic impurities which are detrimental for superconductivity. The tubes were dispersed in dichloroethane and, after 15 min of sonication, they were deposited onto thermally oxidized, strongly doped Si wafers. A tube of 4 μm in length and 16.6 nm in diameter was located using a FE-SEM Zeiss Supra 40. Subsequently, Ti contacts of width 550 nm were made using standard overlay lithography: 10 nm titanium layer in contact with the tube was covered by 70 nm Al in order to facilitate proximity-induced superconductivity in Ti. Last, 5 nm of Ti was deposited to prevent the Al layer from oxidation. The length of the tube section between the contacts was 400 nm. The electrically conducting body of the silicon substrate was employed as a back gate, separated from the sample by 150 nm of SiO_2. An atomic force microscope (AFM) image of our sample is displayed in the inset of Fig. 1.

On our "dipstick" dilution refrigerator (Nanoway PDR50), the samples were mounted inside a tight copper enclosure. The measurement leads were filtered using an RC filter with time constant of 1 μs at 4.2 K, followed by twisted pairs with tight, grounded electrical shields for filtering between the still and the mixing chamber, while the final section was provided by a 0.7-m long Thermocoax cable on the sample holder. In the measurements, current bias was employed via a 100 MΩ room-temperature resistor when searching for supercurrents. The differential resistance $R = dV/dI$ was recorded using standard lock-in techniques. The gap of the contact material was found to be $\Delta_{lead} = 139$ μeV. Normal state results were measured at $B = 0.2$ T.

Our nanotube sample is slightly n-type doped initially, as in our previous measurements on semiconducting MWNTs [12]. The back gate capacitance $C_g = 4$ aF was deduced from the measured gate period of SET oscillations $\Delta V = 40$ mV. The total capacitance of the 4 μm-long nanotube is estimated to be $C_\Sigma = 0.4$ fF, which corresponds to a Coulomb energy of $E_C \sim 2.5$ K. Since the Fermi level of the tube shifts according to $C_g/C_\Sigma e\Delta V_g$, the number of channels can be varied only in the range of $N \simeq 0$ to a few over the employed gate range of $V_g = -10 \cdots +10$ V. Most of the observed changes in resistance $R(V_g)$ are then due to a variation in the distribution of individual transmission coefficients, not from the changes

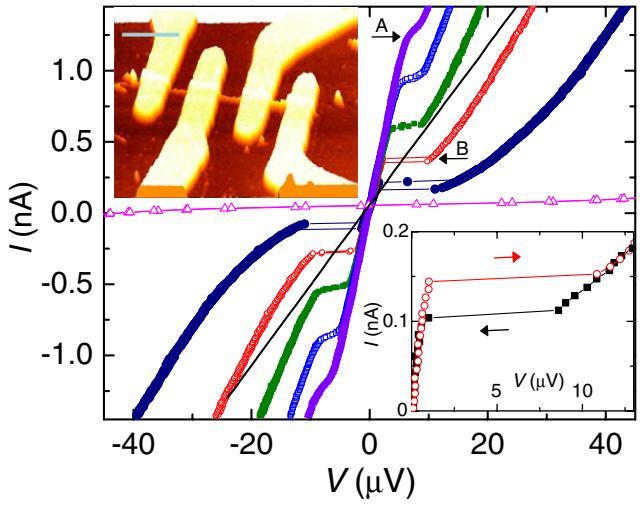

FIG. 1 (color online). Current I as a function of bias voltage V at gate voltage $V_g = 3.214$ V (●); 3.220 V (○); 3.232 V (■); 3.232 V (□); 3.244 V (▲); 3.344 V (△). The solid straight line displays the normal state IV curve measured in a magnetic field of $B = 0.2$ T at $V_g = 3.202$ V. The arrows A and B illustrate the determination of the maximum supercurrent $I_{\rm cm}$ in the nonhysteretic and hysteretic cases. The inset on the lower right illustrates a magnification of the IV curve at $V_g = 3.214$ V, where clear hysteresis is visible and the critical current $I_{\rm cm} = 0.15$ nA. The inset on the upper left displays an AFM image of our sample (scale bar: 1 μm). The data were measured in a two-lead configuration on the middle section at $T = 65$ mK.

in N. There is a part of the change, up to 50% at most (dependent on V_g), that can be attributed to the Kondo effect. Other typical characteristics for our samples are: the mean free path $l_{\rm mfp} \sim 15$ nm and the diffusion constant $D \sim v_F l_{\rm mfp} = 1 \times 10^{-2}$ m^2/s, as deduced from the resistance [13]. This means that a 400 nm long section (see Fig. 1) is expected to be nearly in the long S-NS junction limit. We find several V_g values at which the normal state resistance is in the range $R_n = 15$–20 kΩ. Occasionally, we saw gradual or abrupt shifts of the sample which needed to be corrected by offsetting V_g. This is attributed to variations in the background charge on the order of 0.1–0.3 electrons.

The measured IV curves are illustrated in Fig. 1. The shape is seen to change from a state with linear IV characteristics at small bias to a fully "blockaded" one over $\Delta V_g = 100$ mV. The IV curves in the first category display a pronounced kink, followed by a plateau at voltages in the range of 1–10 μV; at intermediate V_gs even hysteresis is observed. This behavior is identified as proximity-induced superconductivity with the kink or plateau region indicating the maximum measured supercurrent $I_{\rm cm}$. Details of the small bias regime are given in the lower right inset of Fig. 1. There is hysteresis at the intermediate values of the critical currents. After a maximum hysteresis of $\Delta I = I_{\rm cm} - I_{\rm retrap} = 54$ pA at $V_g = 3.214$ V, the hysteresis is seen to diminish as the current is lowered. The maximum product for $I_{\rm cm}R_n = 22\ \mu$eV $\ll \Delta_{\rm lead}$.

According to the RCSJ model, there is hysteresis if the scaled temperature $\Gamma = k_BT/E_J$ is small enough and the McCumber parameter $\beta = (\omega_p RC_{\rm tot})^2 \gg 1$, where ω_p is the plasma frequency, R is the shunt resistance, and $C_{\rm tot}$ is the total capacitance involved in the plasma oscillation. To make an estimate, we take $R = R_J = \frac{dV}{dI} \sim 2$ kΩ from the IV of the junction above the plateau region, $C_{\rm tot} = 400$ fF, and $\omega_p = \sqrt{\frac{2eI_{c0}}{\hbar C_{\rm tot}}}$, we get an estimate $\beta \sim 24$ at $I_{c0} = 5$ nA, where $I_{c0} = \frac{2eE_J}{\hbar}$ is taken at $E_J/k_B = 120$ mK. This estimate is close to critical damping and no hysteresis at $\Gamma \sim 1$ is to be expected [14]. Nevertheless, a suppression of $I_{c0} = 5$ nA down to $I_{\rm cm} = 1.3$ nA takes place by thermal fluctuations. When V_g is tuned, R_J increases more strongly than Γ, leading to the appearance of hysteresis in the IV curves due to a larger value for β. Eventually the increase of Γ with lowering E_J takes over and the hysteresis disappears with decreasing $I_{\rm cm}$ as observed in Fig. 1. Thus, the RCSJ model can qualitatively explain the main characteristics observed in Fig. 1.

The supercurrent branch is found to display a finite resistance which depends only weakly on bias (see the inset of Fig. 1). This weakness of bias dependence distinguishes our results from those of Buitelaar *et al.* [7] and of Jørgenssen *et al.* [6] who both observed a clear peak in the conductance. The dependence of the measured supercurrent $I_{\rm cm}$ on $R_0 = \frac{dV}{dI}|_{V=0}$ as well as on the normal state resistance R_n is given in Fig. 2. $I_{\rm cm}$ could be tuned over 2 orders of magnitude from 1.3 nA down to 10 pA, while the normal state resistance increased only by a factor of 2: from 15 to 35 kΩ. We find that the data can be fitted by a power law behavior $I_{\rm cm} \propto R_0^{-1.35}$.

The relatively large zero bias resistance, $R_0 > 1.4$ kΩ, is in agreement with the ordinary picture of phase diffusion [15,16], which may coexist with hysteretic IV characteristics provided that the environment of the junction is frequency dependent: at ω_p, $Z_{\rm env} \sim Z_0 = 377\ \Omega$ stabilizing phase diffusion, while at low frequencies $Z_{\rm env} \gg Z_0$ [14]. Ingold *et al.* [17] have derived for the zero bias resistance due to phase diffusion

$$R_0 = \frac{Z_{\rm env}}{I_0(E_J/k_BT)^2 - 1}, \qquad (1)$$

where $I_0(x)$ represents a modified Bessel function. Subsequently, Grabert *et al.* have shown that Eq. (1) is rather accurate, within a factor of ~2, even when the quantum fluctuations are included [18]. We stick here to classical phase diffusion because the ratio of thermal to Coulomb energy $k_BT/E_c \sim 50$ owing to large, environmental shunting capacitance.

In Ref. [17], the IV characteristics were derived in the limit $E_J, eV \ll k_BT$ according to which there is a simple relation between I_{c0} and $I_{\rm cm}$:

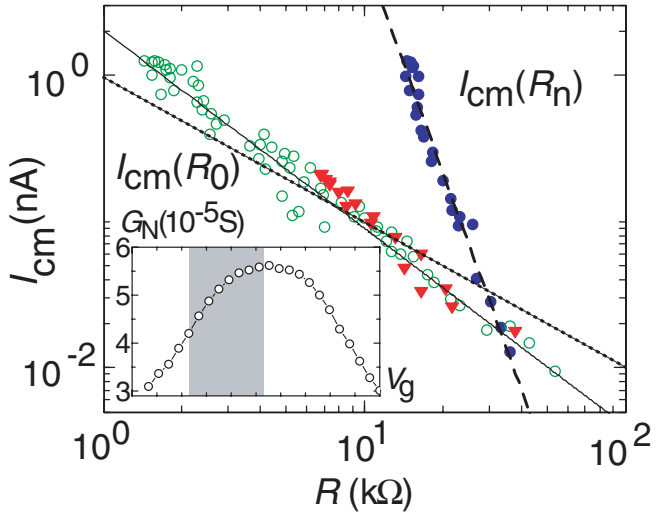

FIG. 2 (color online). I_{cm} *vs.* zero bias resistance R_0 and normal state resistance R_n measured at $T = 80$ mK. The open and filled circles displays R_0 and R_n at $V_g = 3.21 \ldots 3.33$ V, respectively. The filled triangles denote R_0 at $V_g = 5.98 \ldots 6.02$ V. The solid curve is a power law fit with $I_{cm} \propto R_0^{-1.35}$ while the dashed line represents $I_{cm} \propto R_n^{-4.93}$. The dotted curve displays the phase-diffusion relation $I_{cm} \propto R_0^{-1}$ valid at $E_J \ll k_B T$. The inset displays the normal state conductance $G_n = 1/R_n$ vs V_g. The range of the superconducting IV curves in Fig. 1 ($V_g = 3.214$–3.244 V) is indicated by the gray shading.

$$I_{cm} = \frac{E_J}{4k_B T} I_{c0}. \tag{2}$$

Thus, independent of Z_{env}, one expects $I_{cm} \propto E_J^2$ in the overdamped limit. From the maximum value of $I_{cm} = 1.3$ nA, we get $E_J/k_B = 90$ mK at $T = 65$ mK, which is at the limit of applicability of Eq. (2). Equation (1) yields $R_0 \propto E_J^{-2}$ in the limit $E_J \ll k_B T$. Therefore, using Eq. (2), we get $I_{cm} \propto R_0^{-1}$, which is displayed as a dotted line in Fig. 2.

The Josephson energy for a long diffusive junction, without interaction effects, can be calculated from the equation [19,20]

$$I_{C0} = \frac{32}{3 + 2\sqrt{2}} \frac{\epsilon_{Th}}{eR_n} \left(\frac{L}{L_T}\right)^3 \exp\left(-\frac{L}{L_T}\right), \tag{3}$$

which is valid in the limit $\Delta/\epsilon_{Th} \to \infty$ when $T \simeq 3\epsilon_{Th}/k_B$ and where $L_T = \sqrt{\hbar D/2\pi k_B T}$ [21]. In S-N-S structures with tunnel barriers, perturbation analysis of the interacting case has shown that there are logarithmic corrections that reduce Josephson coupling [22], but this theory is not suitable for our case as the contacts have a high transparency. We also neglect resonance effects in our analysis, i.e., the contribution that might be related to Kondo effect.

By combining Eqs. (2) and (3), we obtain an analytical formula for I_{cm} that has only one fitting parameter, namely D (or L_T at certain T). In Fig. 3, we compare this formula with the measured temperature dependence of I_{cm}. The solid curve in Fig. 3 is the result of the fit using $L_T = \sqrt{80 \text{ mK}/T}$ 188 nm. This thermal length corresponds to $D = 2.2 \times 10^{-3}$ m^2/s, yielding $\epsilon_{Th} = 9.0$ μeV [23]. The discrepancy at the lowest temperatures may be an indication that Eq. (2) becomes invalid and numerical analysis based on the Ivanchenko-Zilberman theory should be done. Deviations at the lowest temperatures are also observed between the fit of Eq. (1) and the measured R_0 in Fig. 3.

Figure 4 displays the differential conductance G for the low conductance IV curves of Fig. 1 in the range $V_g = 3.323 \ldots 3.355$ V. A sequence of maxima is seen, which are related to MAR [24,25]. The MAR peaks are more prominent than what we would expect for a long, diffusive contact on the basis of a recent numerical analysis by Cuevas *et al.* [26]. The dashed vertical lines indicate locations for the first Andreev reflection process if it is governed by unrenormalized $\Delta_{lead}/e = 139$ μV. Since Coulomb effects tend to shift MAR peaks upwards in voltage, the gap has to be modified at the interface by 20% downwards, roughly similar to findings by Jørgenssen *et al.* [6] in SWNTs with Al/Ti contacts. Using $\tilde{\Delta} = 0.8\Delta_{lead} = 111$ μeV we find that the main Andreev peaks are located at $\frac{2}{3}\tilde{\Delta}$ and $\frac{2}{5}\tilde{\Delta}$, though the latter one does not coincide exactly to the expected location at $V > 0$.

The weak gate dependence of the MAR lines is quite similar to that found in Ref. [7], where it is assigned to a shift in the resonance condition as V_g is varied [27]. However, since we cannot observe any negative dV/dI, as expected for this situation, we do not believe that our results are related to resonance phenomena, unlike the data in SWNTs [4]. Between $\tilde{\Delta}$ and $2\tilde{\Delta}$ there is an additional peak that may be connected to Thouless energy (ϵ_{Th}). As we approach the supercurrent region by decreasing the V_g, ϵ_{Th} (D) increases and, consequently, the peak should move towards $2\tilde{\Delta}$ [26]. In our experiment, however, the peak

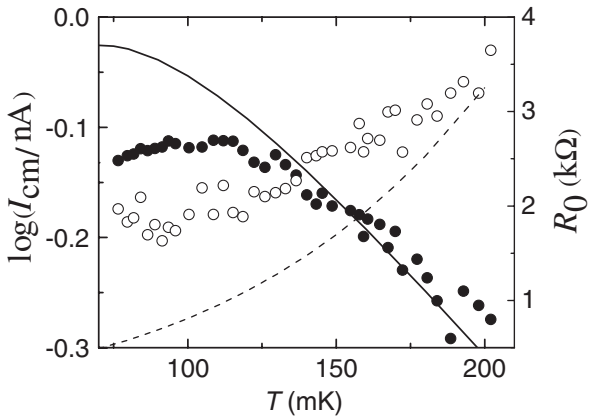

FIG. 3. Temperature dependence of I_{cm} (●) and R_0 (○) measured at $V_g = 3.489$ V. The solid curve is a fit obtained from Eqs. (2) and (3) using $D = 2.2 \times 10^{-3}$ m^2/s, $L = 0.4$ μm, and $R_n = 17$ kΩ. The dashed line displays R_0 calculated from Eq. (1) using $Z_{env} = 400$ Ω and $E_J(T)$ from the above T-dependence fit.

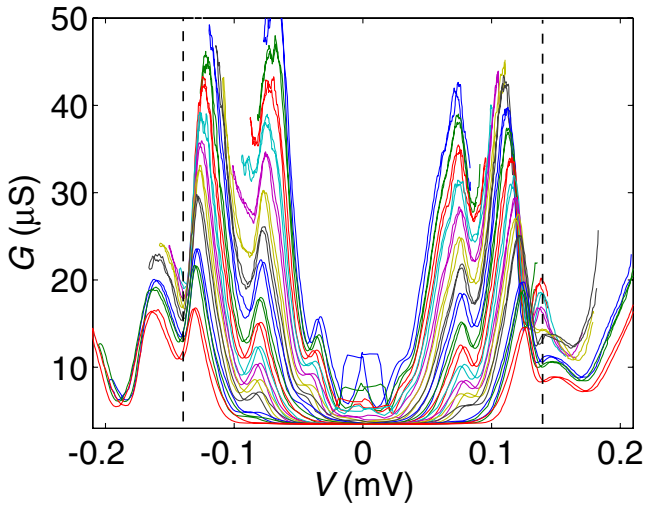

FIG. 4 (color online). Conductance G vs bias voltage V. Gate voltage V_g has been stepped over $V_g = 3.323 \ldots 3.355$ V in steps of 2 mV. The dashed vertical lines indicate locations for the first Andreev reflection process if governed by unrenormalized $\Delta_{\mathrm{lead}}/e = 139$ μeV.

moves towards $\tilde{\Delta}$. Notice also that in the data of Fig. 4, the supercurrent peak near zero bias starts to develop before any signs of higher order Andreev peaks. This seems to contradict with the scenario of Vecino *et al.* [8] who argue that inelastic processes enhance conductance due to higher order MAR processes and lead to IV curves with hysteresis at small bias.

Since the number of transmission channels is rather small in our sample, it is possible that the subgap transport is basically dominated by one single channel. This might result, especially, from the Kondo resonance that is known to play a role in the conductance of good quality MWNTs [7]. In fact, when comparing the shape of the IV curves in Fig. 1 with the calculated IV curves for single-channel S-NS contacts [28] rather good agreement is obtained for the range of transmissions $\tau = 0.3$–0.7. Therefore, even though a description using the model of a long, diffusive junction seems to work well, presumably an analysis based on a set of transmission channels would yield an even better agreement.

In summary, we have observed proximity-induced superconductivity in a diffusive plasma-enhanced chemical vapor deposition-grown MWNT. The Josephson coupling energy could be tuned by V_g via a change in the diffusion constant $D \propto 1/R_n$. The model for long diffusive junctions was successfully employed for calculating the dependence of E_J on R_n and T. The measured IV curves (the zero bias resistance R_0 and maximum supercurrent I_{cm}) could be understood using analysis based on classical phase diffusion, which leads to a decrease of I_{cm} as E_J^2. At $T = 65$ mK, the largest obtained Josephson coupling energy was 0.09 K.

We thank S. Iijima, A. Koshio, and M. Yudasaka for the carbon nanotube material. We wish to acknowledge fruitful discussions with D. Gunnarsson, T. Heikkilä, F. Hekking, P.-E. Lindelöf, M. Paalanen, B. Placais, C. Strunk, and A. Zaikin. This work was supported by the TULE programme of the Academy of Finland and by the EU Contract No. FP6-IST-021285-2.

[1] J. Nygård *et al.*, Nature (London) **408**, 342 (2000).
[2] A. Yu. Kasumov *et al.*, Science **284**, 1508 (1999).
[3] A. Kasumov *et al.*, Phys. Rev. B **68**, 214521 (2003).
[4] P. Jarillo-Herrero *et al.*, Nature (London) **439**, 953 (2006).
[5] A. F. Morpurgo *et al.*, Science **286**, 263 (1999).
[6] H. I. Jorgensen *et al.*, Phys. Rev. Lett. **96**, 207003 (2006).
[7] M. R. Buitelaar *et al.*, Phys. Rev. Lett. **91**, 057005 (2003).
[8] E. Vecino *et al.*, Solid State Commun. **131**, 625 (2004).
[9] J. Haruyama *et al.*, Appl. Phys. Lett. **84**, 4714 (2004).
[10] I. Takesue *et al.*, Phys. Rev. Lett. **96**, 057001 (2006).
[11] A. Koshio *et al.*, Chem. Phys. Lett. **356**, 595 (2002).
[12] F. Wu *et al.*, cond-mat/0606661.
[13] These estimates are given for our regular two-lead sample with a number of channels $N \sim 10$. In our present sample, N depends strongly on the estimate of C_Σ: using a two-lead capacitance for the middle section, $C_\Sigma \sim 0.1$ fF, we end up with $N = 10$–15 in the most investigated range of $V_g = 3$–6 V.
[14] R. L. Kautz and J. M. Martinis, Phys. Rev. B **42**, 9903 (1990).
[15] M. Tinkham, *Introduction to Superconductivity* (McGraw-Hill, New York, 1996), p. 253, ISBN 0-07-064878-6.
[16] Yu. M. Ivanchenko and L. A. Zil'berman, Zh. Eksp. Teor. Fiz. **55**, 2395 (1968) [Sov. Phys. JETP **28**, 1272 (1969)].
[17] G.-L. Ingold *et al.*, Phys. Rev. B **50**, 395 (1994).
[18] H. Grabert *et al.*, Europhys. Lett. **44**, 360 (1998).
[19] A. D. Zaikin and G. F. Zharkov, Sov. J. Low Temp. Phys. **7**, 184 (1981).
[20] P. Dubos *et al.*, Phys. Rev. B **63**, 064502 (2001).
[21] We neglect the effect of interfacial transparency that is known to lower the Josephson coupling in diffusive S-NS stuctures even further. See, M. Yu. Kuprianov and V. F. Lukichev, Zh. Eksp. Teor. Fiz. **94**, 139 (1988) [Sov. Phys. JETP **67**, 1163 (1988)].
[22] C. Bruder *et al.*, Physica (Amsterdam) **B203**, 240 (1994); R. Fazio and G. Schön.
[23] The values for D and ϵ_{Th} would be 10%–20% higher if one would employ a self-consistent numerical evaluation for the product $I_{C0}R_n$. This has been neglected as the main error comes from the lowest order estimate for I_{cm}.
[24] M. Octavio *et al.*, Phys. Rev. B **27**, 6739 (1983).
[25] K. Flensberg *et al.*, Phys. Rev. B **38**, 8707 (1988).
[26] J. C. Cuevas *et al.*, Phys. Rev. B **73**, 184505 (2006).
[27] See, e.g., G. Johansson *et al.*, Phys. Rev. B **60**, 1382 (1999).
[28] D. Averin and A. Bardas, Phys. Rev. Lett. **75**, 1831 (1995); see also, A. Bardas and D. V. Averin, Phys. Rev. B **56**, R8518 (1997).